Dynamical transport properties of NbSe3 with simultaneous sliding of both charge-density waves

A.A. Sinchenko, Pierre Monceau

Dynamical transport properties of $NbSe_3$ with simultaneous sliding of both charge-density waves

A. A. Sinchenko
Kotelnikov Institute of Radioengineering and Electronics of RAS, Mokhovaya 11-7, 125009 Moscow, Russia

P. Monceau
Institut NEEL, CNRS and Université Joseph Fourier, BP 166, 38042 Grenoble, France

(Received 24 October 2012; published 8 January 2013)

Measurements of the nonlinear conductivity in $NbSe_3$ when the high-T and the low-T charge-density waves (CDWs) are simultaneously sliding have been performed. It is shown that the threshold electric field E_{t1} for depinning the high-T CDW increases 4–5 times at the temperature at which the low-T CDW is formed, indicating the strong pinning effect resulting from the interaction between both CDWs. Under application of a radio-frequency (rf) field, Shapiro steps are never observed simultaneously for both CDWs. At the electric field less one than for high-T CDW sliding only Shapiro steps for low-T CDW were observed, and at higher field only Shapiro steps for high-T CDW exist.

DOI: 10.1103/PhysRevB.87.045105 PACS number(s): 71.45.Lr, 72.15.Nj, 72.70.+m

I. INTRODUCTION

$NbSe_3$ is an emblematic quasi-one-dimensional metal with three pairs of metallic chains (types I, II, and III) parallel to the monoclinic b direction.[1] $NbSe_3$ undergoes two successive Peierls transitions: at $T_{P1} = 145$ K with a charge density wave (CDW) essentially on type I chains and at $T_{P2} = 59$ K with a CDW essentially on type II chains.[2] The wave vectors of both CDWs are respectively $\mathbf{Q}_1 = (0,0.241,0)$ and $\mathbf{Q}_2 = (0.5,0.260,0.5)$. The Peierls transitions in this material are not complete and ungapped carriers remain in small pockets at the Fermi level most probably associated with type III chains.[3,4] As a result, $NbSe_3$ keeps metallic properties down to the lowest temperatures. Application of an electric field above a threshold value E_{t1} for high-T CDW and E_{t2} for low-T CDW induces a collective electron transport due to the coherent incommensurate CDW motion.[5,6]

One general question immediately arises when several order parameters coexist in the same material, such as the two CDWs in $NbSe_3$: Are they totally independent or are they interacting with one another? If yes, what is the result and the mechanism of this interaction? Several attempts were already undertaken for answering this question. X-ray scattering measurements on pinned CDWs showed no sign of a lock-in transition[7] which may be envisioned such as

$$2(\mathbf{Q}_1 + \mathbf{Q}_2) \approx (1,1,1). \quad (1)$$

From interlayer tunneling technique[8] it was found that resulting from the low-T CDW formation the CDW gap of the high-T CDW exhibits a 10% decrease below T_{P2}.

As far as the dynamical properties associated with both high-T and low-T CDWs at temperatures $T < T_{P2}$ are concerned, contradictory data were reported. In Refs. 9 and 10 it was indicated that the depinning field E_{t1} of the high-T CDW may saturate below T_{P2}, while according to Ref. 11 E_{t1} continuously grows without any peculiar singularity at T_{P2}.

From high-resolution x-ray scattering in the presence of an applied current below T_{P2}, simultaneous and oppositely directed shifts of the relevant CDW-superlattice components along chains were observed above a threshold current which was identified as the depinning threshold $I_{t1} \sim 10I_{t2}$ for the more strongly pinned high-T CDW.[12] This dynamical decoupling was explained through a sliding-induced charge transfer between the two electronic reservoirs corresponding to the CDW wave vectors $\mathbf{Q}_1$ and $\mathbf{Q}_2$. Using the same technique but in a different context related to switching effects in $NbSe_3$, a dynamical coupling was reported from analysis of the transverse structure of both CDWs.[13] Note that in all these works E_{t1} was not directly determined from nonlinear current-voltage characteristics (IVs) below 60 K but estimated as being the field at which broadband noise (BBN) increased; there is a large uncertainty in this determination (see for instance Fig. 2 in Ref. 12).

Thus, at the present time, there are no complete and reliable measurements describing dynamical properties of $NbSe_3$ in the temperature range corresponding to the coexistence of both CDWs. In the following we report, from current-voltage characteristics (IVs), the observation of the simultaneous sliding behavior for both CDWs. The sliding state of each CDWs is confirmed by the observation of Shapiro steps when a radio-frequency electric field is applied together with the dc electric field. The present work extends the previous report[14] where Shapiro steps were observed separately for each CDW.

II. EXPERIMENTAL TECHNIQUE

The main problem for the determination of the threshold behavior of the high-T CDW at temperature below T_{P2} from IV characteristics is Joule heating. On the one hand, to reduce heating one needs to use samples with high resistance and correspondingly with a small cross section. On the other hand, decrease of the crystal cross section leads to an exponential growth of E_t because of finite size effects.[15] We have found that the compromise between the best thermal conditions and the magnitude of the threshold field takes place by selecting crystals with a thickness (0.4–0.6) μm and for resistance at room temperature in the range 0.5–2.0 kΩ/mm. So, we performed our experiments on three selected high quality $NbSe_3$ single crystals with a thickness indicated above and a width (2–8) μm. The residual resistance ratio of the selected crystals was $R(300\text{ K})/R(4.2\text{ K}) = (50–100)$. The crystals were cleaned in

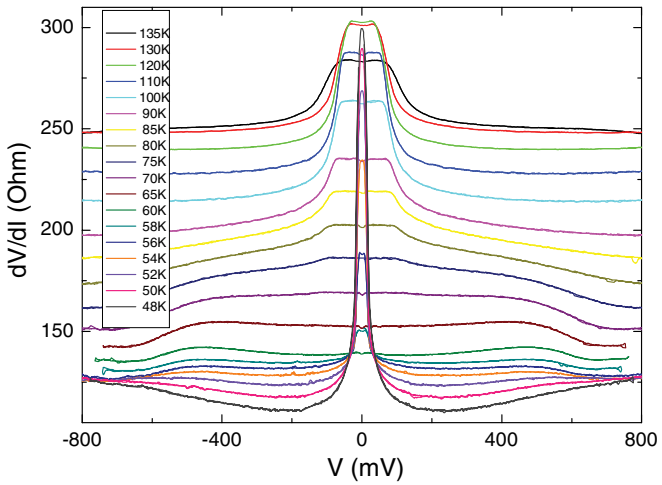

FIG. 1. (Color online) Differential resistance $R_d = dV/dI$ as a function of V at different temperatures varied from 135 to 48 K for sample No. 2.

oxygen plasma and glued on sapphire substrates by collodion. The measurements of IV characteristics and their derivatives have been done in conventional 4-probe configuration. Contacts were prepared from In by cold soldering. The distance between the potential probes was 1 mm for all the samples. For studying nonstationary effects a rf current was superposed on the dc current using the current contacts connected to the rf generator via two capacitors.

III. EXPERIMENTAL RESULTS

In Fig. 1, we have drawn the differential current-voltage characteristics (IVs) in the temperature range 135–46 K for sample No. 2. The qualitatively same characteristics were observed for two other samples. The threshold behavior corresponding to the sliding state of the high-T CDW is clearly seen from 135 K down to 90 K: The behavior is Ohmic for voltage less than a threshold voltage V_{t1}, and for voltages in excess of this value the differential resistance, $R_d = dV/dI$,

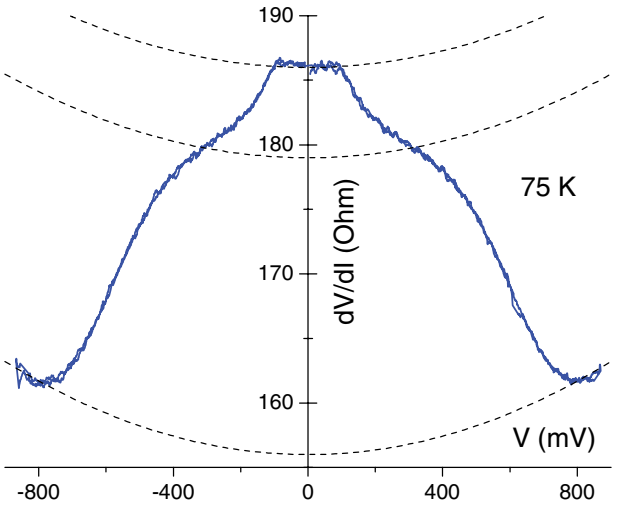

FIG. 2. (Color online) $dV/dI(V)$ dependence at $T = 75$ K for sample No. 2.

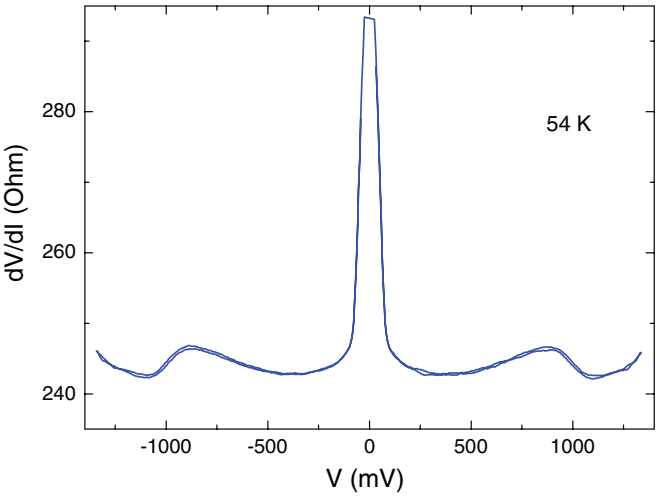

FIG. 3. (Color online) $dV/dI(V)$ dependence at $T = 54$ K for sample No. 3 demonstrating the simultaneous sliding of both CDWs.

decreases sharply. As usual V_{t1} decreases from T_{P1} down to 120 K and monotonically increases at lower temperatures.

Below 90 K a new decrease of R_d appears at a certain voltage V_{t1}^* that is nearly 4–5 times larger than V_{t1} and becomes more and more pronounced in lowering temperature. As an example of such behavior the $dV/dI(V)$ dependence at $T = 75$ K is shown in Fig. 2. When T is reduced, the amplitude of the change in R_d at $V = V_{t1}$ from static to sliding decreases while at $V = V_{t1}^*$ it increases. At $T = T_{P2}$ the first threshold at $V = V_{t1}$ is completely indiscernible, and only the second threshold at $V = V_{t1}^*$ remains. Below T_{P2} we observe the threshold behavior for the low-T CDW at the voltage V_{t2} that is near to 10^2 times less than V_{t1}^*. Figure 3 clearly demonstrates the singularities in the IV curve for sample No. 3 corresponding to the transition into the sliding state of both CDWs at $T = 54$ K.

To prove that nonlinear effects observed in dc IV curves are really associated with CDWs sliding, we have superposed a rf current on the dc current. It is well known that the joint

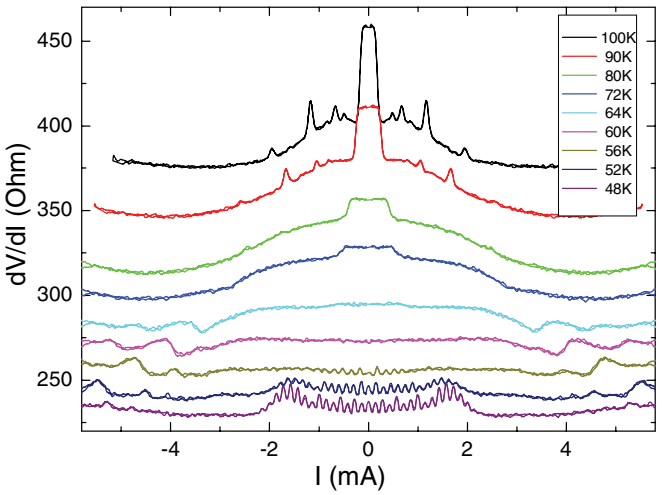

FIG. 4. (Color online) $dV/dI(I)$ dependencies at different temperatures under application of a rf field with a frequency 101 MHz for sample No. 3.

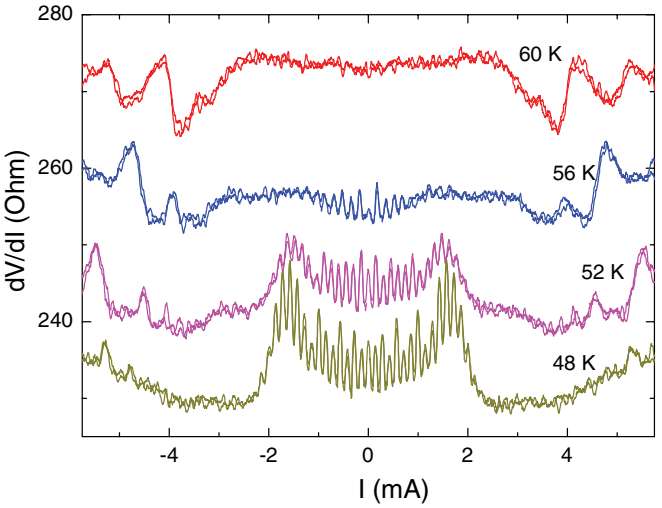

FIG. 5. (Color online) The same as in Fig. 4 at different temperatures below T_{P2}.

application of dc and rf driving fields leads to the appearance of harmonic and subharmonic Shapiro steps in the dc IV characteristics indicating sliding state of CDW.[1,5,6] Differential IV characteristics for sample No. 3 in the temperature range 48–100 K under application of a rf field with a frequency 101 MHz are shown in Fig. 4. The Shapiro steps appear when $E > E_t$ and reflects the synchronization between the internal CDW sliding state and the external frequency. As can be seen, at $T < 70$ K the Shapiro steps corresponding to the high-T CDW are observed at $E > E^*_{t1}$. Note that in the temperature range 60–90 K the Shapiro steps peculiarities are sufficiently weak compared with those at other temperatures.

Below T_{P2} we observe pronounced Shapiro steps for both CDWs as illustrated in Fig. 5 where IV curves at $T = 60$, 56, 52, and 48 K are displayed. Typically the rf amplitude was larger compared with V_{t2} and less than V^*_{t1}. Consequently the dc threshold at V_{t2} is totally suppressed[16] while the threshold at V^*_{t1} is still observable. It is worth noting that Shapiro steps corresponding to the low-T CDW disappear at voltages $V > V^*_{t1}$ and only Shapiro steps associated with the high-T CDW are observable at these voltages.

IV. DISCUSSION

First let us ascertain that the drop of R_d observed at $V = V^*_{t1}$ really corresponds to the sliding of the high-T CDW. It is well known that the fundamental frequency of the narrow-band generation is directly proportional to the CDW current:[1,5,6]

$$\frac{J_{\rm CDW}}{f_0} = c\frac{n(T)}{n(T=0)}, \qquad (2)$$

where $n(T)$ is the number of carriers condensed into the CDW at temperature T, and c is a constant. As far as Shapiro steps are concerned it is necessary to change in Eq. (2) $J_{\rm CDW}$ to $\Delta I_{\rm CDW}$ which corresponds to the difference of CDW current between two neighboring harmonic Shapiro steps. $\Delta I_{\rm CDW}$ can be easy calculated using dc IV characteristics. We have calculated the relation of $\Delta I_{\rm CDW}/f$ for the high-T CDW at temperatures below and above T_{P2} and for the low-T CDW for all measured samples. Estimations for sample No. 2 for the high-T CDW at temperatures $T = 110$ and 54 K and for the low-T CDW at $T = 50$ K with the frequency of the rf field at $f = 53$ MHz are respectively 1.10, 1.17, and 1.28 μA/MHz. In accordance with Ref. 17, we can derive from our experiments that the number of condensed carriers into the CDW state is practically equal for the low- and high-T CDW. Thus, we associate the observed sharp drop in $R_d(V)$ dependencies at $V = V^*_{t1}$ with the transition to the sliding state of the high-T CDW.

Using our dc curves we have also estimated the respective CDW velocities when both CDWs are in a sliding state. Thus for sample No. 3 at $T = 54$ K at the given total transport current $I = 5$ mA, we have evaluated $I_{\rm CDW1} \simeq 0.10$ mA and $I_{\rm CDW2} \simeq 0.83$ mA. Taking for $n = 10^{21}$ cm^{-3} (Ref. 17) and 2.4 μm^2 for the cross-section area, the CDW velocities are respectively 0.25×10^2 cm/s for the low-T CDW and 2.07×10^2 cm/s for the high-T CDW. So, in the state when both CDWs are in the sliding state the velocity of high-T CDW is near one order of magnitude higher than that of the low-T CDW.

In addition we can conclude that at $T < 90$ K the sliding of the high-T CDW is characterized by two threshold fields: E_{t1} and E^*_{t1}. The change in conductivity associated with these two thresholds (indicated by the dashed lines in Fig. 2) is different: When the temperature decreases, the change of conductivity below E_{t1} decreases while that below E^*_{t1} increases. At $T_{P2} = 60$ K there are no more signs of the E_{t1} threshold.

Figure 6 shows the temperature dependencies of threshold fields for high- and low-T CDWs for sample No. 2 in logarithmic scale. The same characteristics were observed for other samples. The $E_{t1}(T)$ demonstrates a conventional behavior. The $E^*_{t1}(T)$ decreases with the temperature decrease from 90 K down to 60 K and remains nearly constant or demonstrates some tendency to increase at $T < 60$ K. The temperature range of the observation of the coexistence between the two thresholds E_{t1} and E^*_{t1} is indicated by the dotted lines. Note that this temperature region corresponds well to that where low-T CDW fluctuations were observed.[18] The temperature dependence of low-T threshold field $E_{t2}(T)$ is in agreement with previous reported data.[11]

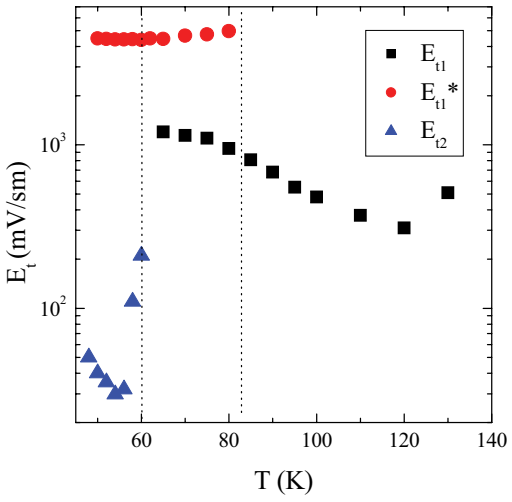

FIG. 6. (Color online) Temperature dependencies the threshold fields $E_{t1}(T)$ (circles), $E^*_{t1}(T)$ (squares), and $E_{t2}(T)$ (triangles) for sample No. 2. Dashed lines indicate the temperature region for fluctuations of the low-T CDW.

We can suggest the following physical picture. Above 60 K the sample may be considered as consisting, in addition to the ordered high-T CDW, of domains of low-T CDW fluctuations. Then the assumption is that these fluctuations strongly pin the high-T CDW. Most probably, the mechanism of this pinning may be a dynamical commensurability pinning between the ordered high-T CDW and fluctuations of low-T CDW.

As a result, in the temperature range between 60 and 90 K the sliding of the high-T CDW exhibits two threshold fields reflecting the mixing of two types of domains. With the temperature growing the size of fluctuation regions decreases and becomes negligibly small at $T > 90$ K where only the phase with E_{t1} has been observed. Inversely, at $T < 60$ K only the phase with E^*_{t1} exists. At temperatures $75 < T < 85$ K both phases are in near equal proportion; as a result the Shapiro steps are essentially smeared at this temperature range.

Another interesting observation of the present work is the unusual structure of Shapiro steps when both CDWs exist simultaneously. As was mentioned above, in such a condition Shapiro steps corresponding to the low-T CDW disappear at voltages $V > V^*_{t1}$ and only Shapiro steps associated with the high-T CDW are observable at these voltages (Fig. 5). Formally it may mean that the motion of the high-T CDW suppresses the narrow-band-noise generation from the low-T CDW. The complete explanation of this effect is missing now.

Recently, a new view on the origin of the narrow band noise generation in CDW compounds was suggested,[14] namely that Shapiro steps in CDW compounds are the result of electronic transport transversely to CDW chains. Such an assumption is based on the theory proposed in Refs. 19 and 20 where it was predicted that the transverse current has a term proportional to the cosine of the difference of phases between the CDW chains. In the case when the CDW slides along one chain but is pinned along neighboring chains, or if the CDW moves with different velocities in different chains, or if the CDW is pinned but phase slippage takes place, then the CDW phase varies with time and alternating tunneling current is generated transversely to the chain direction with a frequency depending on the longitudinal electric field. When an external alternating signal acts on the sample, a resonance can be observed at a fixed V_{tr} if the frequencies of the external and characteristic oscillations coincide. As a result, current Shapiro steps should appear in transverse IVc that was really observed in experiment.[14] In real samples the appearance of an electric potential normal to the transport current exists always and has been attributed to defects and fluctuations of the critical CDW parameters such as threshold electric field or Peierls transition temperature.[21] It is then natural to assume that synchronization of the generated frequencies in $NbSe_3$ will be strongly dependent on the state of all types of chains. Thus, sliding of high-T CDW strongly modifies the transverse current distribution in the sample, and as a result may destroy the synchronization frequencies resulting for low-T CDW sliding. However, to clarify the physical mechanism of this effect new theoretical and experimental investigations need to be performed.

In conclusion, we clearly observed the nonlinear conductivity in current-voltage characteristics of $NbSe_3$, corresponding to simultaneous sliding of both the high-T and the low-T charge-density waves. We show that the interaction between CDWs leads to strong pinning of the high-T CDW and resulting in a 4–5 times increase of threshold electric field. In the temperature range up to 30 K above the second Peierls transition the sliding of the high-T CDW exhibits two thresholds, most probably because of the local fluctuations of the low-T CDW. The superposition of an rf current on the dc current leads to the appearance of Shapiro steps on dc IV curves for low-T CDW at $E < E^*_{t1}$ and for high-T CDW at $E > E^*_{t1}$. Both types of Shapiro steps have never been observed simultaneously.

ACKNOWLEDGMENTS

The authors are thankful to S. V. Zaitsev-Zotov and S. G. Zybtsev for helpful discussions of the experimental results. The work has been supported by Russian State Fund for the Basic Research (No. 11-02-01379-à), and partially performed in the frame of the CNRS-RAS Associated International Laboratory between CRTBT and IRE "Physical properties of coherent electronic states in coherent matter." The support of ANR-07-BLAN-0136 is also acknowledged.

[1] S. Brazovskii, P. Monceau, and N. Kirova, Physica B **407**, 1683 (2012).

[2] G. Grüner, *Density Waves in Solids* (Addison-Wesley, Reading, MA, 1994) .

[3] N. Shima and K. Kamimura, in *Theoretical Aspects of Band Structure and Electronic Properties of Pseudo-One-Dimensional Solids*, edited by K. Kamimura (Reidel Publishing Company, Dordrecht, The Netherlands, 1985), p. 231.

[4] A. A. Sinchenko, R. V. Chernikov, A. A. Ivanov, P. Monceau, Th. Crozes, and S. A. Brazovskii, J. Phys.: Condens. Matter **21**, 435601 (2009).

[5] *Charge Density Waves in Solids*, edited by L. Gor'kov and G. Grüner (Elsevier Science Publishers B. V., Amsterdam, The Netherlands, 1985).

[6] P. Monceau, Adv. Phys. **61**, 325 (2012).

[7] R. M. Fleming, C. H. Chen, and D. E. Moncton, Colloque C3, J. Phys. (France) **44**, C3-1651 (1983).

[8] A. P. Orlov, Yu. I. Latyshev, A. M. Smolovich, and P. Monceau, JETP Lett. **84**, 89 (2006).

[9] J. C. Gill, J. Phys. F **10**, L81 (1980).

[10] J. Richard and P. Monceau, Solid State Commun. **33**, 635 (1980).

[11] R. M. Fleming, Phys. Rev. B **22**, 5606 (1980).

[12] A. Ayari, R. Danneau, H. Requardt, L. Ortega, J. E. Lorenzo, P. Monceau, R. Currat, S. Brazovskii, and G. Grübel, Phys. Rev. Lett. **93**, 106404 (2004).

[13] Y. Li, D. Y. Noh, J. H. Price, K. L. Ringland, J. D. Brock, S. G. Lemay, K. Cicak, R. E. Thorne, and Mark Sutton, Phys. Rev. B **63**, 041103(R) (2001).

[14] A. A. Sinchenko, P. Monceau, and T. Crozes, Phys. Rev. Lett. **108**, 046402 (2012).

[15] J. McCarten, D. A. DiCarlo, M. P. Maher, T. L. Adelman, and R. E. Thorne, Phys. Rev. B **46**, 4456 (1992).

[16] A. Zettl and G. Grüner, Phys. Rev. B **29**, 755 (1984).
[17] J. Richard, P. Monceau, and M. Renard, Phys. Rev. B **25**, 948 (1982).
[18] Ch. Brun, Zhao-Zhong Wang, P. Monceau, and S. Brazovskii, Phys. Rev. Lett. **104**, 256403 (2010).
[19] S. N. Artemenko and A. F. Volkov, Sov. Phys. JETP **60**, 395 (1984); JETP Lett. **37**, 368 (1983).
[20] S. N. Artemenko, JETP **84**, 823 (1997).
[21] A. A. Sinchenko, P. Monceau, and T. Crozes, JETP Lett. **93**, 56 (2011).